

UTRA FDD Simulator: A Rigorous Implementation of 3GPP Specifications

Ernesto L. Andrade Neto¹, Ailton A. Shinoda², Marcelo E. Pellenz³, Michel D. Yacoub¹
¹UNICAMP, Campinas SP / ²UEL, Londrina PR / ³PUCC, Curitiba PR - Brazil

Abstract - In this paper we describe a rigorous implementation of an UTRA FDD simulator. The simulator strictly abides by the 3GPP standards implementing the detailed transmission chain. We analyze the results of a comprehensive simulation of the UTRA FDD downlink traffic channels. We evaluate the UTRA FDD performance under power control and multiple access interference. The reference channel model used for the simulations is entirely based on the COST 259 channel model and provides a realistic scenario for radio propagation. The simulator aims at being used as a test bed for new technologies based on the 3GPP standards. The results shown here provide an insight into how to assess the actual UTRA FDD data channels performance.

I. INTRODUCTION

The 3G wireless systems are designed to support a great variety of wideband services such as high-speed Internet access and high quality image transmission, in addition to the conventional wireless services. One of the most promising radio transmission technology standards within IMT-2000 is based on ETSI's Universal Mobile Telecommunication System (UMTS) and is known as UMTS Terrestrial Radio Access (UTRA) [1]. UTRA is certainly a tough competitor as a 3G technology due to its compatibility with existing GSM networks, which hold the largest share in the cellular market.

The access scheme for UTRA is Direct Sequence Code Division Multiple Access (DS-CDMA). UTRA comprises two different modes namely: Frequency Division Duplex (FDD) and Time Division Duplex (TDD). In this work, we describe the implementation of an UTRA simulator operating in the FDD mode. This simulator aims at being used as a test bed to design new technologies and techniques for UTRA FDD. It is built as add-on modules for SimulinkTM so as to allow for an easy integration of the UTRA FDD models and the algorithms and techniques developed within MatlabTM. The simulator implements in *detail* and *rigorously* all the aspects of the UTRA FDD downlink, as specified in 3GPP Recommendations (e.g., [2-5]).

In section 2, we introduce the UTRA FDD forward link transmission chain. In section 3, we discuss the COST 259 channel model. In section 4, we discuss the simulation

configurations concerning the simulation setups for single user operation, multiple access interference (MAI), and transmission power control (TPC). In section 5, we illustrate some results for the proposed simulation setups and analyze the UTRA FDD performance. In section 6, we draw the final comments and conclusions about the actual status of this work.

II. UTRA FDD DOWNLINK

This section describes the UTRA FDD downlink as implemented in the simulator. The simulation of the UTRA FDD downlink is divided in two main components: 1) the implementation of the 3GPP standards for the transmitter and 2) the implementation of a suitable receiver matched to the transmitter specifications. The other relevant aspect within the simulation is the channel model to be used. In this work, the COST 259 model is included. Figure 1 shows the framework of the implemented UTRA FDD downlink simulator based on the 3GPP standards.

In UTRA FDD radio interface, the information is spread over approximately a 5 MHz bandwidth with a chip rate of 3.84 Mchip/s. In the simulator two dedicated downlink Physical Channels are modeled: Dedicated Physical Data Channel (DPDCH) and Dedicated Physical Control Channel (DPCCH) [3]. The DPDCH is used to convey the Dedicated Channel (DCH) Transport Channel whereas the DPCCH is used to carry physical control information represented by the Pilot Bits, Transport Format Combination Indicator (TFCI) Bits, and Transmission Power Control (TPC) Bits. Both DPDCH and DPCCH channels are time multiplexed within a radio frame of 10 ms, which contains 15 slots. Given that the transmission rate is 3.84 Mchip/s, the total number of chips per radio frame and per slot is 38400 and 2560 respectively. A slot corresponds to one power control period and is 0.6666... ms long. The total number of bits per slot ranges from 10 to 1280 with the spreading factor correspondingly varying from 512 to 4. The channel symbol rate is half of the channel bit rate, both rates obtained immediately before spreading.

The DPDCH used for speech and the DPCCH are encoded with 1/3 rate constraint length 9 convolutional code as described in [4]. The DPDCH conveying the data channels are encoded with 1/3 rate turbo coding according

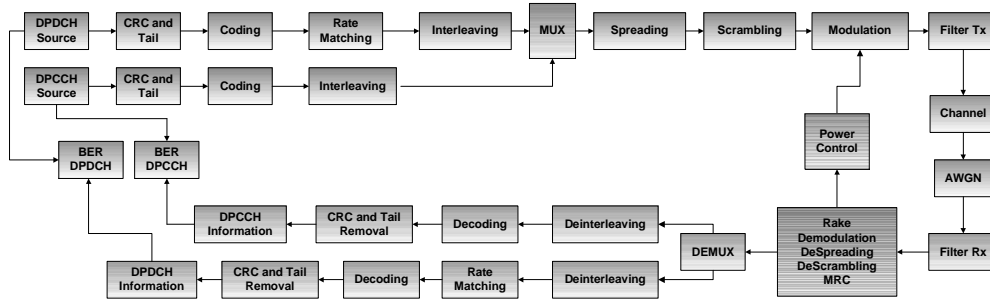


Figure 1: UTRA FDD downlink simulator structure.

to [4]. Once the Physical Channels are formatted they are ready for transmission. The transmission of the Physical Channels consists of two processes: spreading and modulation. Spreading consists of the following operations: channelization and scrambling. The channelization operation transforms each symbol into a number of chips, given by the spreading factor, thus increasing the signal bandwidth. In the scrambling operation, the resulting spread signal is further multiplied by a scrambling code. The chip sequence generated by the spreading process is QPSK modulated. In the modulation process, the real part and the imaginary part of the spread signal are independently pulse shaped and multiplied by the in-phase carrier and the quadrature carrier, respectively. The pulse shaping method uses a root-raised cosine filtering with a roll-off factor of 0.22. In the spreading process, the binary Physical Channels are represented by real-valued sequences, in which the binary value 0 is mapped onto the real value +1 and the binary value 1 is mapped onto the real value -1. The channelization codes used in UTRA are known as Orthogonal Variable Spreading Factor (OVSF) codes. The OVSF codes preserve the orthogonality between channels of different rates and spreading factors [5].

The next step in the simulation process is the transmission of the processed data through the wireless channel. The channel model used is based on COST 259 [6]. The channel consists of a channel bank generated with different parameters according to COST 259 model. After the slot propagates through the channel white gaussian noise (AWGN) is added to the information signal.

The second part of the implemented UTRA FDD downlink simulation deals with the receiver aspects. At the reception end, the received signal is processed by the reception filter, which is matched to the transmission filter. A rake receiver is then implemented. Currently the rake receiver performs maximal ratio combining (MRC) using a combination of an adjustable number of rake fingers. For the rake receiver operation the following has been assumed: 1) the rake fingers may perform an ideal or an erroneous estimation of the multipath delay, and 2) the rake fingers may also perform an ideal or an erroneous estimation of the multipath channel phase. The rake receiver always tracks the strongest multipath signals

during the simulation. Within each rake finger despreading and descrambling are performed.

After MRC, symbol decision is carried out, and the received packet is reassembled and the demultiplexed onto DPCCH and DPDCH. DPCCH and DPDCH are then deinterleaved, rate matched, and decoded by convolutional and turbo decoders, respectively. The next process is the extraction of CRC and the tail bits for both channels. The resulting data sequence for each channel is compared to the original transmitted data sequence to check for errors.

Multiple Access Interference (MAI) is introduced by means of a structured way rather than by treating it as AWGN. MAI is implemented by generating the signals for a number of interfering mobile stations (MSs) within the system. Each interfering user has its own control channel (DPCCH) and one data application (DPDCH).

When power control is enabled, in a slot per slot basis, the rake receiver also estimates the average received signal to interference ratio (SIR) per slot. The power control algorithm, as implemented in the simulator [7], increases the transmitted power whenever the estimated SIR drops below a pre-established threshold. The power control process also limits the minimum and maximum transmitted power. When power control is used combined with MAI all the interfering mobiles also have their own power control loops.

III. CHANNEL

The use of generally accepted channel models has been very beneficial for the development of the mobile communications standards and equipment. Several limitations of the GSM and similar channel models have been identified [8]. In order to increase the usefulness of the channel models while aiming at the same general acceptance, COST 259 has developed a new directional channel model with the following properties [8]: 1) channel directionality for use with adaptive antennas and space diversity; 2) inclusion of channel polarization; 3) detailed characterization of the wideband channel; 4) representation of large-scale variations modeling the effect of mobiles moving continuously through a cell site; 5) introduction of location dependence, implying that a

mobile returning to its starting point after moving around within a cell will experience the same channel condition; 6) definition of a single-cell model, meaning that multiple links to a single base station can be modeled simultaneously with correlations depending on the geographical separation of the mobiles.

In the implementation of the link level simulator, we apply channel banks generated within COST 259 directional channel model to simulate several radio propagation scenarios. The channels generated by COST 259 Directional Channel Impulse Responses (DCIRs) have the general expression shown in equation (1).

$$h(\vec{r}, \tau, \Omega) = \sum_{l=1}^{L(\vec{r})} h_l(\vec{r}, \tau, \Omega) \quad (1)$$

Here, \vec{r} denotes the location of the RX antenna, and τ is the delay variable. The direction of arrival is characterized by the parameter Ω . The latter may be described in terms of its azimuth angle ϕ and its elevation angle ϑ , where ϑ is positive above the horizontal plane. DCIR is decomposed into a finite number L of components, each of which corresponds to an impinging wave. The components may embody a specular and/or a diffuse part. Note that in (1) directions of departure and polarization have been omitted.

In order to better characterize the COST 259 channels, we estimate the delay spread, as defined in equations (2) and (3), and the Rician factor, as defined in (4), in accordance with [9]. In particular, as far as the results to be shown here are concerned, two of the COST 259 radio propagation environments, namely, Typical Urban and Rural, are used. The delay spread is given by

$$\sigma_\tau = \sqrt{\frac{\sum_{l=1}^L (\tau_l - \tau_a)^2 \cdot |h_l|^2}{\sum_{l=1}^L |h_l|^2}} \quad (2)$$

$$\text{where, } \tau_a = \frac{\sum_{l=1}^L \tau_l |h_l|^2}{\sum_{l=1}^L |h_l|^2} \quad (3)$$

$|h_l|^2$ and τ_l are the power and delay of l -th multipath respectively. The Rician factor can be approximated by

$$K = 10 \cdot \log_{10} \left(\frac{|h_1|^2}{\left(\sum_{l=1}^L |h_l|^2 \right) - |h_1|^2} \right) \quad (4)$$

The Rician factor gives a “shape factor” for the channel environment impulse response [9]. Table I shows the values of delay spread and Rician factor for the environments used in the simulations.

TABLE I
DELAY SPREADS AND RICIAN FACTOR FOR THE CHANNELS
GENERATED ACCORDING TO COST259 DCIR MODEL

Scenario	Delay Spread (μ s)			Rician Factor (K) dB		
	Mean	Min.	Max.	Mean	Min.	Max.
Typical Urban	0.77	0.48	1.28	-3.44	-8.13	3.23
Rural	0.30	0.03	0.60	4.01	-4.65	22.25

Examples of the channel power delay profiles for the channels used in the simulations generated with the COST 259 model [8] can be seen in Figures 2-5. For the results to be shown here we compare Typical Urban and Rural environments including mobility scenarios such as low mobility (5 km/h), medium mobility (50 km/h), and high mobility (120 km/h).

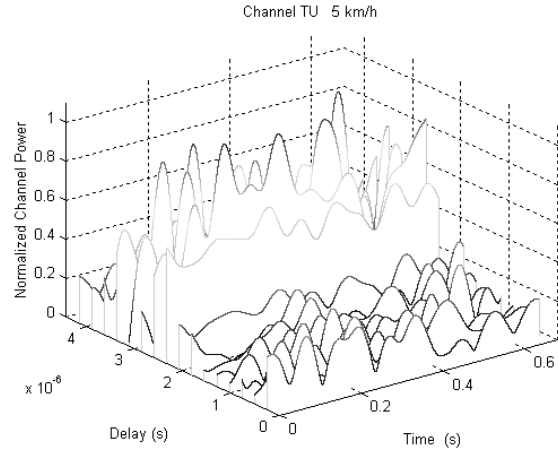


Figure 2: Power Delay Profile for the Typical Urban environment at 5 km/h.

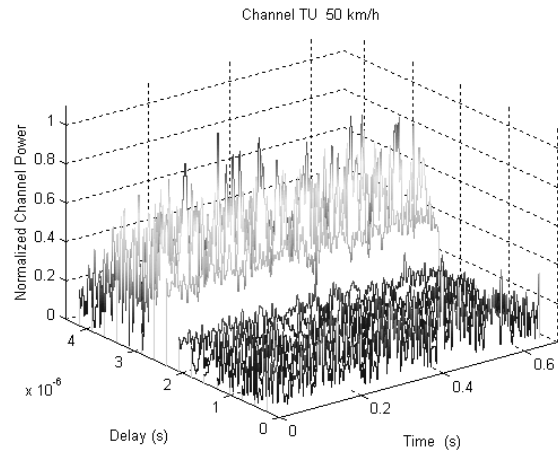


Figure 3: Power Delay Profile for the Typical Urban environment at 50 km/h.

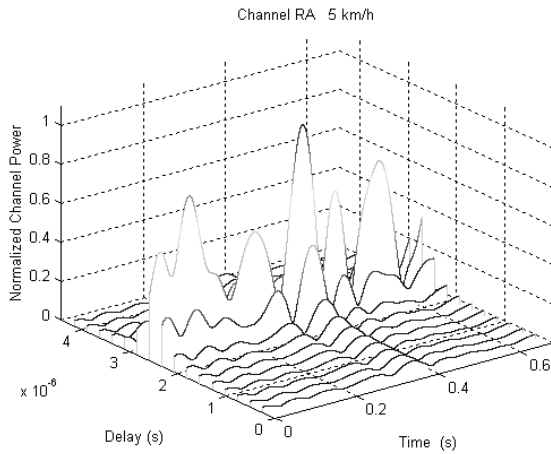


Figure 4: Power Delay Profile for the Rural environment at 5 km/h.

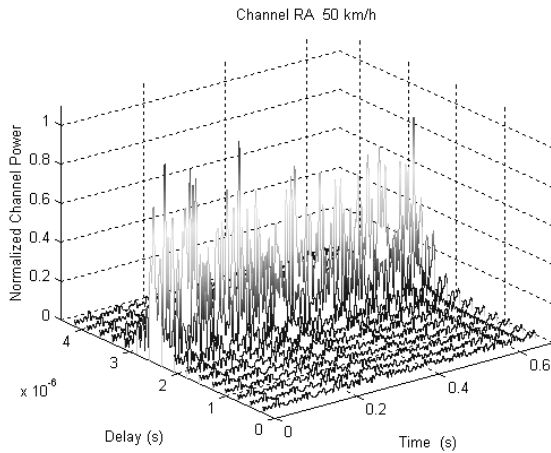


Figure 5: Power Delay Profile for the Rural environment at 50 km/h.

IV. SIMULATION SETUP

This section describes the simulation methodology used to assess UTRA FDD downlink performance given in terms of Bit Error Rate (BER). During the simulation, data are transmitted continuously in a slot-by-slot basis over the COST 259 channels. The simulation process includes fast fading, path loss, and shadow fading. For the results shown here the channel banks are generated as if an MS is moving within the macro-cell with velocities of 5 km/h, 50 km/h, and 120 km/h. The multipath profiles have a maximum delay spread of 4.2 μ s. The simulated macro-cell radius is 2 km.

The selection of data rates to be simulated is chosen to match the data rates of the IMT-2000 macro-cell data channels of 64 kbps and 128 kbps. No antenna diversity technique is considered for the simulation. The data rates, symbol rates, and spreading factors for the DPDCHs and DPCCHs used in the simulations are shown in Table II.

TABLE II
BIT RATES, SYMBOL RATES, AND SPREADING FACTORS FOR FORWARD LINK UTRA FDD DEDICATED DATA AND CONTROL CHANNELS

Channel	Bearer Rate kb/s	Symbol Rate ks/s	Spreading Factor
DPDCH/ DPCCH	64	32	32
	128	64	16

The rake receivers used for the simulations have three fingers to perform MRC. The rake receivers are feed with an imperfect channel estimation to perform MRC. The channel estimation is chosen to be ideal only at the beginning of the slot and the receiver does not correct the variations along the time slot. At reception, turbo decoding use hard decision. The turbo decoder algorithm employs a log MAP metric for symbols decision and performs eight interactions before decision.

The power control algorithm when enabled allows the BS to increase the target MS power in order to compensate for the MAI. In the MAI simulations, the target mobile undergoes a mean interference level that corresponds to a 50 % load in the system. It means that the number of admitted users is half of the spreading factor for the same data rate in the cell. For instance, in the 128 kbps data scenario we include 8 interferers. The target mobile estimates the received downlink DPCCH/DPDCH power of the connection to be power controlled. Simultaneously, the mobile estimates the received interference. The Signal to Interference Ratio (SIR or alternatively E_b/I_0) measurement scheme plays an important role to achieve accurate power control. The system described in this paper use pilot and data symbols for the SIR measurement. In order to estimate E_b/I_0 , E_b is evaluated after the despreading/descrambling of the received signal by the target MS. The I_0 estimation is similar to the E_b estimation, but the short code employed at reception for power measurement is different from all the short codes employed by the target and interfering MSs. The mean E_b/I_0 is measured on a slot-by-slot basis and compared with the target SIR. This is used to increase or decrease the power transmitted to the target MS.

In the structured MAI model each interfering MS has its own power control loop. The same procedure is employed by the target MS, the only difference being the method to increase or decrease the interfering power. For the target MS if the measured E_b/I_0 is higher than the target E_b/I_0 the power is decreased by 1 dB, otherwise the power is decreased by 1 dB. For the simulated interfering MSs, at each time slot the probability that a given interferer increases or decreases its own power by 1 dB is drawn from a uniform distribution with probability $p=0.5$ for each event.

V. SIMULATION RESULTS

This section describes the simulation results obtained for the single user, multiple access interference and

multiple access interference plus power control simulation setups.

Figure 6 to Figure 11 show some results for BER as a function of E_b/N_0 for both Typical Urban and Rural environments. Figure 6 shows the BER performance for single user 64 kbps and 128 kbps data channels in the Typical Urban environment. We note that, as expected, the slower the speed the better the performance. The exception for this is for the MS moving at 5 km/h when E_b/N_0 increases above 5 dB. This is due to increased influence of the long fading periods experimented by the mobile at that low speed.

Figure 7 shows the BER performance results for single user 64 kbps and 128 kbps data channels in the Rural environment. Note that although the distribution of the energy of the multipaths signals between the environments differs the behavior is similar to the Typical Urban environment.

Figure 8 shows the BER performance with multiple access interference for the 64 kbps and 128 kbps data channels for the Typical Urban environment. Note that the slower the velocity the better the BER performance.

Figure 9 shows the BER performance with multiple access interference for the 64 kbps and 128 kbps data channels for the Rural environment. Note that the behavior according to the velocity is similar to the single user case however the BER drop occurs at higher values of E_b/N_0 .

In Figure 6 through Figure 8, we observe that the 128 kbps data channel, although with a lower spreading factor, performs better than the 64 kbps data channel in both environments. In these scenarios, the multipaths and MAI dominate and the observed performance difference is due to the higher coding gains obtained with the use of a larger code block size [10] for the 128 kbps data channel. In Figure 9 the performance gain of the 64 kbps data channel over the 128 kbps data channel reflects the Rural environment better channel conditions.

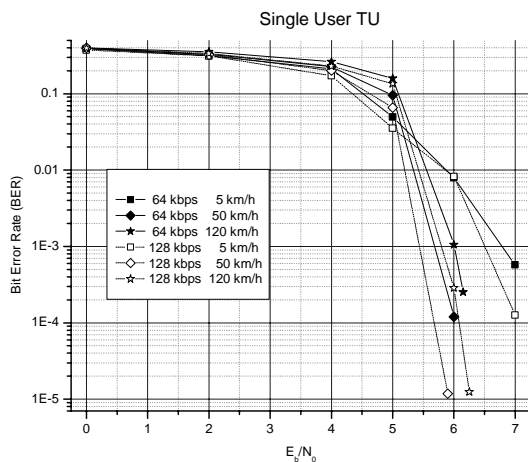


Figure 6: Error rates for the Typical Urban environment with single user.

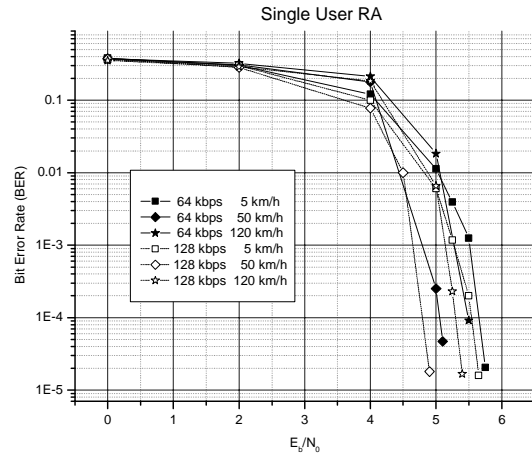


Figure 7: Error rates for the Rural environment with single user.

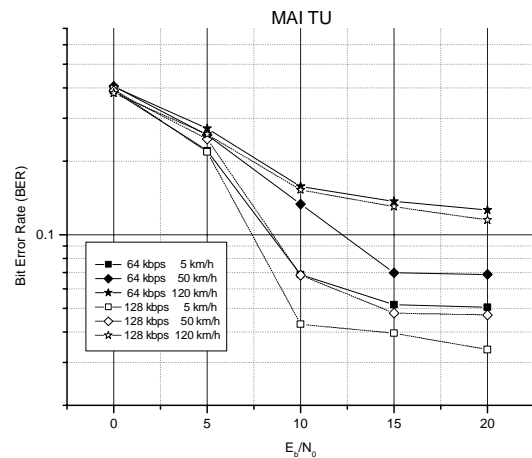


Figure 8: Error rates for the Typical Urban environment with MAI.

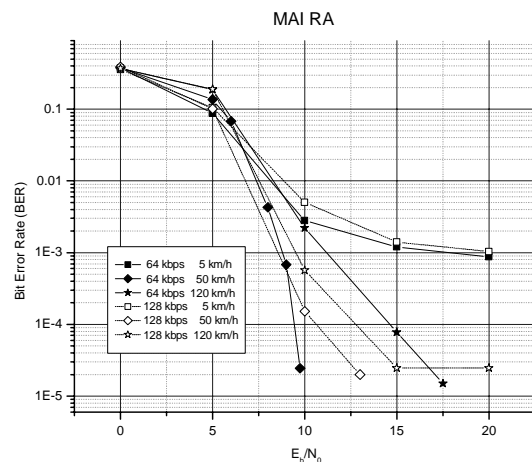


Figure 9: Error rates for the Rural environment with MAI.

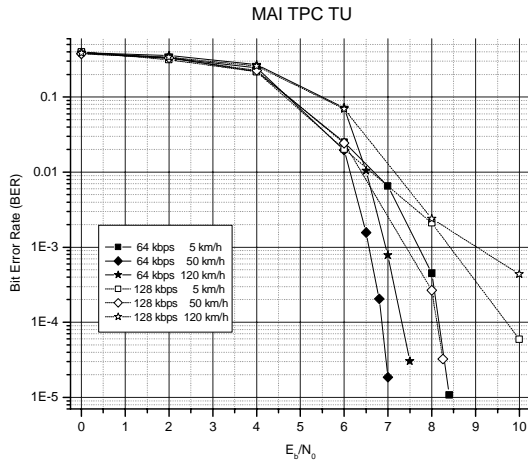


Figure 10: Error rates for the Typical Urban environment with MAI and TPC.

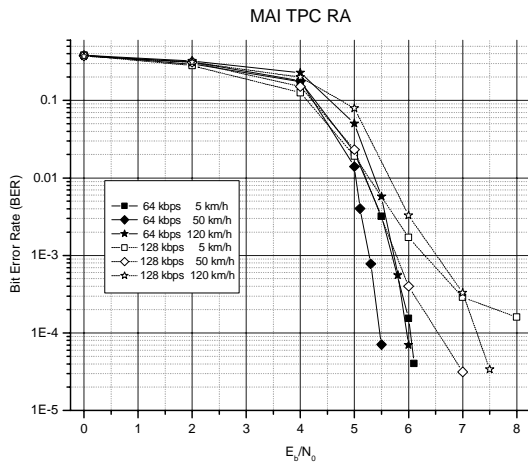


Figure 11: Error rates for the Rural environment with MAI and TPC.

Figure 10 shows the BER performance with MAI plus power control for the 64 kbps and 128 kbps data channels in the Typical Urban. We observe that, below a certain value of E_b/N_0 , the BER performance is as expected (the higher the velocities the lower the BER). Above such a value, with the application of the power control algorithm inversion points are achieved and the performance is not as expected any longer. Certainly, this is an interesting point of investigation, which leads one to better explore other power control mechanisms.

Figure 11 shows the BER performance with MAI plus power control for the 64 kbps and 128 kbps data channels in the Rural environment. The results are similar to the former however occurring at lower values of E_b/N_0 .

In Figure 10 and Figure 11, for the MAI plus TPC scenario, as opposed to Figure 6 to Figure 8 for the single user and MAI scenarios, the 64 kbps data channel displays a BER performance improvement when compared to 128

kbps data channel. This is due to the fact that the power control mitigates the MAI and reduces the multipath interference observed by the target MS.

One interesting point that can be observed in some of the illustrations (Figures 6 to 7 and Figures 10 to 11) is the effect of using turbo encoding. In these illustrations, we note that there is a sudden drop on the BER at a certain E_b/N_0 level, this point corresponding to that above which the turbo decoder becomes effective.

VI. CONCLUSION

The implementation of the UTRA FDD forward link has been successfully carried out. For such an implementation the Simulink environment has been utilized. The Simulink simulation environment provides a quick and simple interface that can be used for a reliable insight into the UTRA FDD downlink behavior.

We observe that the use of turbo coding plays a decisive role in high data rate transmission performance. In addition, power control algorithms must be carefully designed so as to be effective in mitigating MAI.

The observed differences in the BER performance according to the MS velocity are mainly dependent on the radio propagation environment conditions.

We have shown that the simulator can be efficiently employed as a test bed for new technologies based on the 3GPP standards.

ACKNOWLEDGMENTS

This work has been fully supported by Ericsson Telecomunicações S/A under contract N^o 11/00 and 23/00.

REFERENCES

- [1] M. D. Yacoub, "Wireless Technology: Protocols, Standards and Techniques", CRC Press, 2001.
- [2] 3GPP TS 25.211, V3.5.0 (2000-12), "Physical channels and mapping of transport channels onto physical channels (FDD)"
- [3] 3GPP TR 25.944, V3.3.0 (2000-12) "Channel coding and multiplexing examples"
- [4] 3GPP TS 25.212 V3.5.0 (2000-12), "Multiplexing and modulation (FDD)".
- [5] 3GPP TS 25.213 V3.4.0 (2000-12), "Spreading and modulation (FDD)"
- [6] "Wireless Flexible Personalized Communications: COST 259: European Co-operation in Mobile Radio Research, Editor Luis M. Correia, John Wiley, 2001.
- [7] S. Seo, T. Dohi, and F. Adachi, "SIR-Based Transmit Power Control of Reverse Link for Coherent DS-CDMA Mobile Radio", IEICE Transactions on COM, vol. E81-B, no. 7, pp. 1508--1516, July 1998.
- [8] "The COST 259 Directional Channel Model – a stochastic model for spatial wideband channel", Ericsson Internal Report, 2001.
- [9] B. Allen, J. Webber, P. Karlsson, M. Beach, "UMTS Spatio Temporal Propagation Trial Results", IEE ICAP, pp. 497-501, April, 2001.
- [10] S. Dolinar, D. Divsalar, F. Pollara, "Code Performance as a Function of Block Size", TMO Progress Report 42-133, NASA JPL, May 15, 1998.